

## Molecular Impact of the Membrane Potential on the Regulatory Mechanism of Proton Transfer in Sensory Rhodopsin II

Xiue Jiang,<sup>†</sup> Martin Engelhard,<sup>‡</sup> Kenichi Ataka,<sup>\*,§,||</sup> and Joachim Heberle<sup>§</sup>

*Department of Chemistry, Biophysical Chemistry (PC III), Bielefeld University, 33615 Bielefeld, Germany, MaxPlanck Institute of Molecular Physiology, 44221 Dortmund, Germany, Department of Physics, Experimental Molecular Biophysics, Freie Universität Berlin, 14195 Berlin, Germany, and Japan Science and Technology Agency, 102-0075, Tokyo, Japan*

Received March 18, 2010; E-mail: ataka@zedat.fu-berlin.de

**Abstract:** Metabolism establishes a potential difference across the cell membrane of every living cell which drives and regulates secondary ion and solute transfer across membrane proteins. Unraveling the effect of the membrane potential on the level of single molecular groups of the membrane protein was long hampered by the lack of appropriate analytical techniques. We have developed Surface Enhanced Infrared Difference Absorption Spectroscopy (SEIDAS), a highly sensitive vibrational technique for surface analysis, for the study of solid-supported monolayers of orientated membrane proteins. Here, we present spectroscopic data on vibrational changes of sensory rhodopsin II from *Natronomonas pharaonis* (NpSR II). The application of the electrode potential provides a voltage drop across the NpSR II monolayer through the Helmholtz double layer that mimics the cellular membrane potential. IR difference spectra indicated a shift of the photostationary equilibrium from an M and O mixture toward an M dominant equilibrium. The shift of positive to negative potential exhibited similar effects on the light-induced SEIDA spectra as the increase in pH. This effect is explained in terms of local pH change raised by the compensation of excess charge from the electrode. As we have shown earlier (Jiang, et al. *Proc. Natl. Acad. Sci. U.S.A.* **2008**, *105* (34), 12113–12117), the application of an electric field opposite to the physiological proton transfer from the retinal Schiff base to its counterion Asp75 leads to the selective halt of the latter. However, when the solution pH is much higher than 5.8, that is, when the proton releasing group at the extracellular side is ionized, proton transfer of Asp75 becomes insensitive to the electric field exerted by the electrode. We infer that the deprotonation of the proton release group creates a local polar environment surrounding Asp75 as a consequence of hydrogen-bonding rearrangements that exceeds the energy of the external dipole. Our results reveal a molecular model for the physiological regulation of the photocycle of NpSR II by the potential drop across the membrane which came about by the interplay between the change in local pH at the membrane surface and the external electric field.

### Introduction

*Natronomonas pharaonis* sensory rhodopsin II (NpSR II, also called *pharaonis phoborhodopsin*<sup>1</sup>) is the primary light sensor for the photophobic response of these Halobacteria. The membrane protein is activated by green light and propagates a signal to its cognate transducer protein, HtrII, which through downstream signal transduction processes eventually leads to the cell swimming away from blue-green light.<sup>2</sup> SR II is a member of the growing family of microbial rhodopsins that act as light-driven ion pumps, sensors, and channels.<sup>3,4</sup> The polypeptide of SR II folds into the membrane in the form of

seven  $\alpha$ -helices and harbors all-*trans* retinal as a chromophore that is covalently bound via a Schiff base linkage to a lysine residue of the apoprotein. The cyclic photoreaction is initiated by electronic excitation of the cofactor which creates a conformational strain to the protein. The conformational change relaxes back to the original state through several structural intermediate states. These features are common to all microbial rhodopsins such as bacteriorhodopsin (BR), halorhodopsin (HR), sensory rhodopsin (SR I and SR II), and channelrhodopsin. The crystal structure of SR II has been solved with the help of cubic phase crystallization, even in complex to its cognate transducer.<sup>5</sup> The high-resolution structure sets the basis for studies on the reaction mechanism.

The photocycle intermediates in NpSR II comprises intermediates K, M, and O, termed in analogy to those in BR. The

<sup>†</sup> Bielefeld University.

<sup>‡</sup> MaxPlanck Institute of Molecular Physiology.

<sup>§</sup> Freie Universität Berlin.

<sup>||</sup> Japan Science and Technology Agency.

- (1) Hirayama, J.; Imamoto, Y.; Shichida, Y.; Kamo, N.; Tomioka, H.; Yoshizawa, T. *Biochemistry* **1992**, *31* (7), 2093–2098.
- (2) Hoff, W. D.; Jung, K. H.; Spudich, J. L. *Annu. Rev. Biophys. Biomol. Struct.* **1997**, *26*, 223–258.
- (3) Klare, J. P.; Chizhov, I.; Engelhard, M. *Results Probl. Cell Differ.* **2008**, *45*, 73–122.

- (4) Radu, I.; Bamann, C.; Nack, M.; Nagel, G.; Bamberg, E.; Heberle, J. *J. Am. Chem. Soc.* **2009**, *131* (21), 7313–7319.

- (5) Gordeliy, V. I.; Labahn, J.; Moukhametianov, R.; Efremov, R.; Granzin, J.; Schlesinger, R.; Büldt, G.; Savopol, T.; Scheidig, A. J.; Klare, J. P.; Engelhard, M. *Nature* **2002**, *419* (6906), 484–487.

potential presence of the L and N intermediate is still controversial for NpSR II.<sup>6</sup> It is of remarkable relevance that NpSR II is able to pump protons from the cytoplasmic to the extracellular side in the absence of transducer, albeit with lower pumping efficiency than BR.<sup>7,8</sup> The absence of transducer also leads to a deceleration of the photocycle kinetics ( $\tau = 0.1-1$  s depending on the experimental conditions<sup>9-11</sup>).

FTIR spectroscopy is a powerful tool to study the molecular events when NpSR II undergoes the photocycle. IR difference spectra between the ground state and the K-, M-, O-intermediates were resolved either by steady-state cryogenic trapping<sup>6,12</sup> or by time-resolved step-scan spectroscopy.<sup>13-15</sup> The spectra of NpSR II in the K-intermediate revealed the structural similarity to BR with respect to the polyene chain of the chromophore isomerized from all-*trans* to 13-*cis*.<sup>12</sup> The K-state decays to the M intermediate, in which proton transfer from the retinal Schiff base to its counterion Asp75 takes place. The following O intermediate is the last detectable intermediate of the photocycle prior to the return to the initial ground state. In this state, the retinal Schiff base is reprotonated and restored in all-*trans* conformation, while Asp75 is still protonated.<sup>12</sup> The O intermediate decays in the late millisecond time-range which is similar to the M state.<sup>9,10,16</sup> Thus, photostationary conditions lead to mixtures of both intermediates.

Despite these achievements, an essential component is scarcely considered for the functional study of membrane protein, namely, the impact of the membrane potential.<sup>17</sup> In every living cell, ion pumps, channels, and transporters create and employ the energy of the potential difference. It is evident that membrane proteins are influenced by the ubiquitous potential difference across the cellular membrane in which they are embedded. Yet, it is difficult to elaborate the impact of the membrane potential on the molecular level because of experimental difficulties. Manor et al. investigated effects of membrane potential on photochemical reaction of SR I, BR and HR enveloped in lipid vesicles by UV/vis flash spectroscopy.<sup>18</sup> They reported that hyper-polarization increases the lifetime of the M intermediates of BR and SRI-HtrI complex, and retards the photocycle of HR. Here, we used IR spectroscopy to study the molecular impact of the membrane potential on the reaction mechanism, which provides more detailed atomic/molecular

view on biological reactions. When it comes to FTIR difference spectroscopy, conventional transmission methods or even attenuated total reflection (ATR) requires stacks of membrane proteins to be sampled (>200 membrane layers), to achieve sufficient signal-to-noise in the spectra. Such experimental limitations hinder IR spectroscopic studies that target the functionality of electron- or potential-triggered proteins. We solved this problem by immobilizing membrane protein monolayers on a gold electrode, as biomimetic models of physiological relevance.<sup>19,20,21</sup> In this novel approach, the solid gold electrode supplies a voltage drop across the adsorbed protein layer to mimic the membrane potential. The lack of sensitivity of conventional FTIR spectroscopy for the detection of protein monolayers is compensated by the application of surface enhanced infrared absorption spectroscopy (SEIRAS).<sup>22</sup> SEIRAS employs the acute enhancement of vibrational bands from molecules that are adsorbed on nanostructured gold thin films. The challenge to acquire the minute signals that arise from structural changes of the protein monolayer was met by integrating SEIRAS and reaction-induced difference spectroscopy (SEIDAS, surface enhanced infrared difference absorption spectroscopy).<sup>23</sup> In our recent paper, we have demonstrated that SEIDAS provides the sensitivity to resolve the impact of the electric field across the SR II monolayer on the level of atoms and bonds.<sup>19</sup>

In this work, we investigated the consequences of the potential drop on the photoreaction of the SR II monolayer. A highly orientated SR II monolayer is formed on the surface of a gold electrode via the specific affinity of the His-tagged protein with the Ni-NTA modified solid surface. Once adhered to the surface, the SR II monolayer is reconstituted into a lipidic environment and the resulting protein-lipid layer is subjected to a trans-membrane voltage that drops off at the protein-coated working electrode (gold). Thus, gold is not only used as the plasmonic substrate for generating an enhanced electromagnetic field along the surface, but is also employed as a chemically modified electrode. With the membrane mimicry, we have studied in this contribution the interplay between the photoinduced reaction and the applied membrane potential across the membrane protein SR II by *in situ* detection with SEIDAS. It is demonstrated with this approach that the change of the molecular structure of SR II can be directly monitored during its photoinduced reaction under the influence of the external potential. These results set the basis to develop a molecular model for the physiological regulation of the photocycle of NpSR II by the membrane potential.

## Experimental Section

The surface of the gold thin film, that was employed in SEIRAS, was modified by nickel chelating nitrilo-triacetic acid (Ni-NTA) according to published procedures.<sup>21,22</sup> His-tagged sensory rhodopsin II from *N. pharaonis* (NpSR II) was expressed and purified as described.<sup>24</sup> Binding of NpSR II via the C-terminal His-tag to the

- (6) Furutani, Y.; Iwamoto, M.; Shimono, K.; Kamo, N.; Kandori, H. *Biophys. J.* **2002**, *83* (6), 3482-3489.
- (7) Schmies, G.; Engelhard, M.; Wood, P. G.; Nagel, G.; Bamberg, E. *Proc. Natl. Acad. Sci. U.S.A.* **2001**, *98* (4), 1555-1559.
- (8) Schmies, G.; Luttenberg, B.; Chizhov, I.; Engelhard, M.; Becker, A.; Bamberg, E. *Biophys. J.* **2000**, *78* (2), 967-976.
- (9) Chizhov, I.; Schmies, G.; Seidel, R.; Sydor, J. R.; Luttenberg, B.; Engelhard, M. *Biophys. J.* **1998**, *75* (2), 999-1009.
- (10) Miyazaki, M.; Hirayama, J.; Hayakawa, M.; Kamo, N. *Biochim. Biophys. Acta* **1992**, *1140* (1), 22-29.
- (11) Mironova, O. S.; Efremov, R. G.; Person, B.; Heberle, J.; Budyak, I. L.; Büldt, G.; Schlesinger, R. *FEBS Lett.* **2005**, *579* (14), 3147-3151.
- (12) Furutani, Y.; Iwamoto, M.; Shimono, K.; Wada, A.; Ito, M.; Kamo, N.; Kandori, H. *Biochemistry* **2004**, *43* (18), 5204-5212.
- (13) Engelhard, M.; Scharf, B.; Siebert, F. *FEBS Lett.* **1996**, *395* (2-3), 195-198.
- (14) Hein, M.; Wegener, A. A.; Engelhard, M.; Siebert, F. *Biophys. J.* **2003**, *84* (2), 1208-1217.
- (15) Bergo, V. B.; Spudich, E. N.; Rothschild, K. J.; Spudich, J. L. *J. Biol. Chem.* **2005**, *280* (31), 28365-28369.
- (16) Iwamoto, M.; Hasegawa, C.; Sudo, Y.; Shimono, K.; Arais, T.; Kamo, N. *Biochemistry* **2004**, *43* (11), 3195-3203.
- (17) Rivas, L.; Hippler-Mreyen, S.; Engelhard, M.; Hildebrandt, P. *Biophys. J.* **2003**, *84* (6), 3864-3873.
- (18) Manor, D.; Hasselbacher, C. A.; Spudich, J. L. *Biochemistry* **1988**, *27* (16), 5843-5848.

- (19) Jiang, X.; Zaitseva, E.; Schmidt, M.; Siebert, F.; Engelhard, M.; Schlesinger, R.; Ataka, K.; Vogel, R.; Heberle, J. *Proc. Natl. Acad. Sci. U.S.A.* **2008**, *105* (34), 12113-12117.
- (20) Ataka, K.; Richter, B.; Heberle, J. *J. Phys. Chem. B* **2006**, *110* (18), 9339-9347.
- (21) Ataka, K.; Giess, F.; Knoll, W.; Naumann, R.; Haber-Pohlmeier, S.; Richter, B.; Heberle, J. *J. Am. Chem. Soc.* **2004**, *126* (49), 16199-16206.
- (22) Ataka, K.; Heberle, J. *Anal. Bioanal. Chem.* **2007**, *388* (1), 47-54.
- (23) Osawa, M. In *Handbook of Vibrational Spectroscopy*; Chalmers, J. M., Griffiths, P. R., Eds.; Wiley: Chichester, 2002; pp 785-799.
- (24) Hohenfeld, I. P.; Wegener, A. A.; Engelhard, M. *FEBS Lett.* **1999**, *442* (2-3), 198-202.

Ni-NTA modified gold surface was carried out by incubating a 4  $\mu\text{M}$  solution of protein in 0.02% dodecylmaltoside (DDM, pH = 8.0, 20 °C, 0.5 M NaCl, 10 mM bis-Tris-propane buffer). Reconstitution of the membrane protein monolayer into a lipid bilayer was performed by detergent removal and parallel addition of polar lipid from the purple membrane in the presence of Biobeads. For light-induced IR difference spectroscopy, SR II was illuminated by a light-emitting diode (LED, Luxeon Star) with the emission maximum at 497 nm and an intensity of about 10 mW/cm<sup>2</sup>.<sup>19</sup>

Details of the spectroscopic setup used for SEIRAS have been described elsewhere.<sup>25</sup> Briefly, a thin film of gold is wet-chemically deposited on the surface of a triangular Si internal reflection element (IRE), and mounted on a home-built single reflection ATR unit. IR absorption spectra were recorded on an IFS 66v/S FT-IR spectrometer (Bruker). To achieve sufficient signal-to-noise level to detect an absorbance signal as weak as  $10^{-6}$ , typically 1024 scans were accumulated with 4 cm<sup>-1</sup> spectral resolution for each light-induced difference measurement. This procedure was repeated more than 100 times and spectra were averaged. We have not applied any spectral treatment, such as baseline correction, to the data. After the gold film/Si IRE was mounted on the spectro-electrochemical cell, the gold film was immersed in a solution containing 4 M NaCl and 50 mM phosphate buffer. The gold film served as working electrode through copper contact, while Ag/AgCl with 3 M KCl and Pt mesh were used as a reference and counter electrodes, respectively. Potentials are given with respect to the normal hydrogen electrode (NHE:  $E_{\text{NHE}} = E_{\text{Ag/AgCl}} + 0.2 \text{ V}$ ). It is noted that the given potential is that applied to the electrode. The resulting electric field that drops off across the membrane cannot be quantified due to the unknown dielectric properties of the solid-supported membrane. Yet, we assume that the voltage drops off in the Helmholtz double layer where the solid-supported membrane is located.

## Results

**Light-Induced Surface-Enhanced Infrared Difference Absorption Spectroscopy (SEIDAS) on the SR II Monolayer in the Presence of an Applied Electrical Field.** A monolayer of SR II was stepwise assembled along the solid gold surface and reconstituted in lipids under *in situ* observation by SEIRAS. Light excitation induces conformational changes in the photo-receptor SR II which were recorded by the SEIDAS. Figure 1 shows the corresponding SEIDA spectra of SR II when the electrode potential was varied between +0.6 and -0.8 V (at a bulk pH of 5.8). The negative bands refer to the dark state which was taken as a reference, whereas positive bands correspond to the vibrations of intermediates in the photostationary state which was established under continuous illumination with blue-green light. Prominent difference bands were categorized in spectral regions of the cofactor retinal plus amide II (1500–1600 cm<sup>-1</sup>), amide I bands of the peptide bonds (1620–1680 cm<sup>-1</sup>), and bands of carboxylic acids and amide side chain (1690–1770 cm<sup>-1</sup>).<sup>13,26</sup> Generally, difference spectra were almost invariant versus the applied potential in the range between +0.4 and -0.4 V. However, the spectra changed significantly when the potential is < -0.5 V. In the carboxylic acid region, a single peak at 1765 cm<sup>-1</sup> (+) is observed at -0.8 V. The shoulder at 1757 cm<sup>-1</sup> (+) increased with potential increase and became almost equal in intensity to the peak at 1765 cm<sup>-1</sup> at -0.4 V. The bands at 1764 and 1757 cm<sup>-1</sup> are assigned to the C=O stretching mode of Asp75, indicating proton transfer to the carboxylate of the aspartate which was the counterion of the

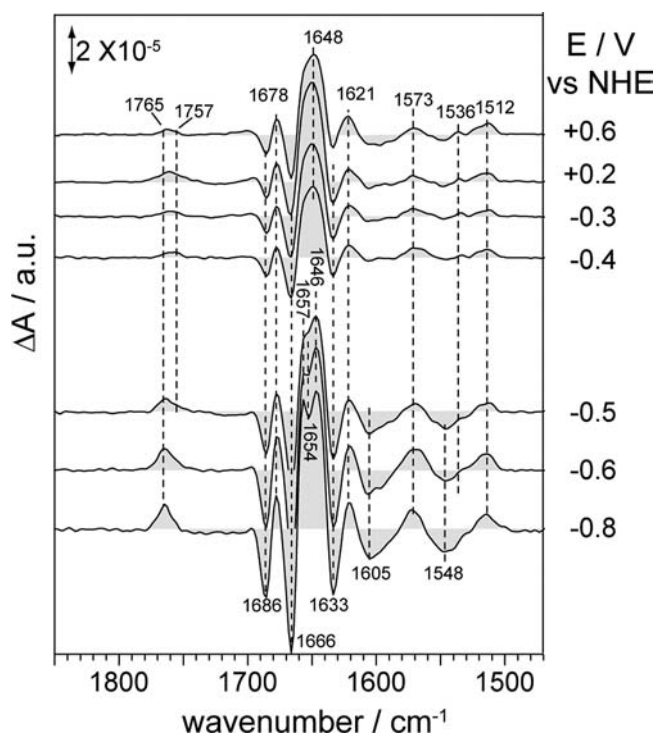


**Figure 1.** Light-induced surface-enhanced infrared difference (SEIDA) spectra of a monolayer of sensory rhodopsin II from *N. pharaonis* (NpSR II). Difference spectra were recorded between the dark and the lit states under continuous illumination with blue-green light ( $\lambda_{\text{max}} = 497 \text{ nm}$ ). Various electrode potential were applied to the membrane monolayer in the range between +0.6 and -0.8 V as specified on the right-hand of the panel. Potentials are given versus the normal hydrogen electrode. The pH of the electrolyte was set to 5.8.

protonated Schiff base of ground-state retinal.<sup>6,12,13</sup> In the amide I region, major changes occurred at around 1650 cm<sup>-1</sup>. At potentials > -0.4 V, a single broad peak is observed which is maximal at 1648 cm<sup>-1</sup> (+). This band splits into three peaks at 1657 (+), 1654 (-), and 1646 cm<sup>-1</sup> (+) at potential more negative than -0.4 V. Large changes are observed as well in the cofactor/amide II region at <1600 cm<sup>-1</sup> when difference spectra below and above -0.4 V are compared. Two new negative bands became noticeable at 1605 cm<sup>-1</sup> and 1548 cm<sup>-1</sup> at  $E < -0.4 \text{ V}$ , while both disappear at  $E > -0.4 \text{ V}$ .

The band at 1548 cm<sup>-1</sup> (-) has been assigned to the ethylenic C=C stretching vibration of the all-*trans* retinal. The small positive absorption at 1536 cm<sup>-1</sup> (shifting from 1548 cm<sup>-1</sup> in the ground state) in the spectra at  $V > +0.4 \text{ V}$  represented the C=C stretch of retinal in the O intermediate.<sup>12</sup> The intensity is very low in our monolayer experiments which is due to the surface selection rule of SEIRAS, in which only vibrational modes perpendicular to the surface are enhanced.<sup>27</sup> It is evident from the crystal structure of SR II<sup>28</sup> that the retinal chain which parallels the C=C dipole moment vector is tilted by about 60° away from the surface normal. This orientation reduces the observed intensity of the ethylenic mode as compared to conventional ATR or transmission experiments (see spectra in refs 6, 12, 13). The appearance of the C=O band at 1757–1765 cm<sup>-1</sup> indicated that the counterion of Asp75 is protonated.<sup>12</sup> Taken together, these marker bands suggested that the photo-

(25) Ataka, K.; Heberle, J. *J. Am. Chem. Soc.* **2004**, *126* (30), 9445–9457.  
 (26) Krimm, S.; Bandekar, J. *Adv. Protein Chem.* **1986**, *38*, 181–364.

(27) Osawa, M.; Ataka, K.; Yoshii, K.; Nishikawa, Y. *Appl. Spectrosc.* **1993**, *47* (9), 1497–1502.  
 (28) Luecke, H.; Schobert, B.; Lanyi, J. K.; Spudich, E. N.; Spudich, J. L. *Science* **2001**, *293*, 1499–1503.



stationary state at  $E > -0.4$  V is dominated by the contribution of the O intermediate.

The presence of the bands at  $1548\text{ cm}^{-1}$  (–) and  $1765\text{ cm}^{-1}$  (+) in the spectra at  $E < -0.4$  V together with the absence of the band at  $1757\text{ cm}^{-1}$  (+) suggested that the M intermediate dominated at these applied potential regions. This is supported by the stronger negative band at  $1548\text{ cm}^{-1}$  (–) (ethylenic mode of ground-state SR II) which is not compensated by the band at  $1536\text{ cm}^{-1}$  (ethylenic mode of the O state of SR II) suggesting that the retinal chromophore is in 13-*cis* configuration. The single peak at  $1765\text{ cm}^{-1}$  (+) suggested a homogeneous hydrogen-bonding environment of protonated Asp75 as expected for a pure M state without admixture from the O intermediate. It is unclear if the splitting of the  $1648\text{ cm}^{-1}$  peak into peaks at  $1657$ ,  $1654$ , and  $1645\text{ cm}^{-1}$  relates to the predominant presence of the M intermediate. This splitting was difficult to be observed and appeared only as a weak shoulder at  $1654\text{ cm}^{-1}$ .<sup>13</sup> It was suggested that the C=N stretching mode from the terminal guanidyl group of Arg72 may appear at around  $1660\text{ cm}^{-1}$  when  $\text{Cl}^-$  is bound to the extracellular side.<sup>29</sup> Further investigation will be necessary for understanding of this issue as a future task.

It is known from detailed studies on BR that the presence of the O state is highly dependent on the pH with the predominance at acidic pH.<sup>30</sup> It has been suggested that the rate of conversion of the M to the O state in SR II is dependent on pH, that is, the decay of the M intermediate is accelerated at  $\text{pH} < 6$  while the O decay is prolonged at lower pH.<sup>9,16,31</sup> As a consequence, the O intermediate is accumulated at lower pH. Thus, we examined the pH dependence of the M/O equilibrium in SR II by performing light-induced SEIDAS at various pH of the bulk solution but at constant potential (open circuit potential OCP of  $+0.2$  V vs NHE,<sup>19</sup>). Striking similarities were observed between the potential dependence (Figure 1) and the pH dependence of the light-induced difference spectra (Figure 2). At pH values lower than 5.5, the spectra in Figure 2 are almost identical to those at  $E > -0.4$  V in Figure 1. The following marker bands indicated the presence of the O state in both series of difference spectra: (i) equal contribution of the C=O stretching band at  $1765\text{ cm}^{-1}$  and  $1757\text{ cm}^{-1}$ , (ii) a single peak at  $1648\text{ cm}^{-1}$ , and (iii) lack of C=C ethylenic band at  $1548\text{ cm}^{-1}$ . As the pH increases above 6, contributions of the band at  $1757\text{ cm}^{-1}$  disappeared and the C=O vibrational band merges into a single peak centered at  $1765\text{ cm}^{-1}$ . Concomitant to pH increase, the peak at  $1648\text{ cm}^{-1}$  split to  $1657$ ,  $1654$ , and  $1646\text{ cm}^{-1}$  and a negative peak appears at  $1548\text{ cm}^{-1}$ . These spectral features corresponded to those observed in Figure 1 as for spectra at  $E < -0.4$  V. Thus, the observed spectra in Figure 2 at lower pH than 5.5 are assigned to the predominance of the O intermediate, while those at  $\text{pH} > 6.0$  are dominated by the presence of the M intermediate. It is evident from the spectral comparison between the series of pH dependent and voltage dependent light-induced IR difference spectra that the M state is the longest-living intermediate at  $\text{pH} > 6.0$  or at  $E < -0.4$  V, while the O decay is slower at  $\text{pH} < 6.0$  or at  $E > -0.4$  V.

It is worthwhile to note that the potential-dependent difference spectra of the lipid reconstituted SR II monolayer differ from

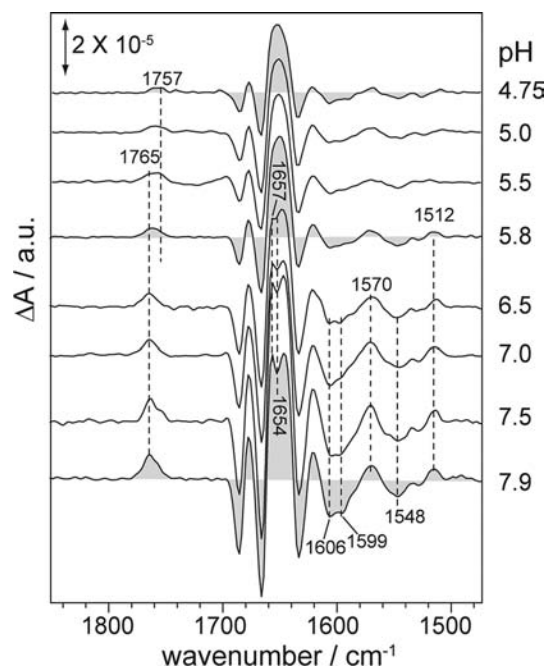


**Figure 2.** Light-induced SEIDA spectra of the NpSR II monolayer recorded at different solution pH (quoted at the right-hand of the Figure). Spectra are taken at open circuit potential ( $+0.2$  V).

those previously reported on SR II monolayer in detergent but recorded under otherwise identical conditions (see Figure S1). A clear deviation from the difference spectrum of SR II in detergent is the appearance of a strong negative band at  $1544\text{ cm}^{-1}$  at  $E > -0.4$  V. From our above results, we can now assign this difference to the dominance of the M intermediate in the absence of lipid even at positive potential region. This result contrasts the lipid reconstituted SR II monolayer where the O intermediate dominated in the same potential region. Nevertheless, there are spectral features in the two difference spectra of the reconstituted and the nonreconstituted SR II monolayer that are inconsistent. The most prominent difference bands in the SEIDA spectra of nonreconstituted SR II does not exhibit splitting of the amide I band ( $1657$ ,  $1654$ , and  $1646\text{ cm}^{-1}$ ) which is the major characteristic in the difference spectrum of the M state of lipid reconstituted SR II monolayer. The appearance of differences in the amide I region suggests that there is a considerable change in the protein structure induced by lipid reconstitution. Although it was reported that lipid–protein interaction notably affected the photocycle kinetics and structure of NpSR II,<sup>32–34</sup> such differences have not been resolved by conventional FT-IR difference spectroscopy where light-induced difference spectra were invariant toward reconstitution with lipids.<sup>6,12</sup> Thus, our SEIDA spectra reveal, for the first time, the effect of the lipid on the structure of SR II.

#### Influence of Applied Electric Field on the Proton Transfer.

Our previous study on nonreconstituted SR II monolayer showed that internal proton transfer is strongly influenced by the applied electrode potential.<sup>19</sup> In the nonreconstituted NpSR II monolayer, the relative intensity of the C=O vibrational band of

(29) Kitade, Y.; Furutani, Y.; Kamo, N.; Kandori, H. *Biochemistry* **2009**, *48* (7), 1595–1603.

(30) Zscherp, C.; Heberle, J. *J. Phys. Chem. B* **1997**, *101* (49), 10542–10547.

(31) Iwamoto, M.; Sudo, Y.; Shimono, K.; Araiso, T.; Kamo, N. *Biophys. J.* **2005**, *88* (2), 1215–1223.

(32) Sudo, Y.; Yamabi, M.; Iwamoto, M.; Shimono, K.; Kamo, N. *Photochem. Photobiol.* **2003**, *78* (5), 511–516.

(33) Iwamoto, M.; Shimono, K.; Sumi, M.; Koyama, K.; Kamo, N. *J. Phys. Chem. B* **1999**, *103* (46), 10311–10315.

(34) Klare, J. P.; Bordignon, E.; Doebber, M.; Fitter, J.; Kriegsmann, J.; Chizhov, I.; Steinhoff, H. J.; Engelhard, M. *J. Mol. Biol.* **2006**, *356* (5), 1207–1221.

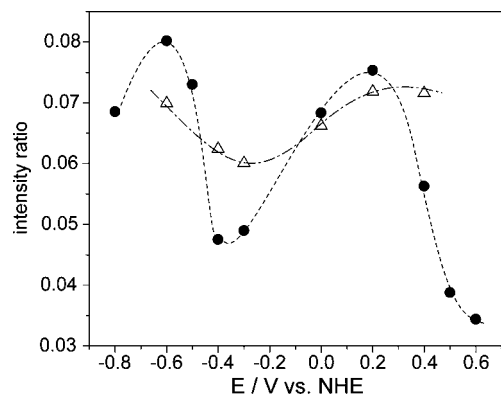


**Figure 3.** Plot of the integrated intensity ratio of the C=O stretching vibrational band of Asp75 at 1764 and 1757  $\text{cm}^{-1}$  versus the applied potential. Integrated band area of Asp75 was normalized to the integrated area of the amide I band at 1668–1635  $\text{cm}^{-1}$  for each spectrum. Data were taken from the experiments at pH 5.8 (filled circles; ●) and pH 7.0 (open triangles;  $\Delta$ ).

Asp75 proportionally decreased as the potential became lower, which indicates a suppression of the proton transfer at negative potential at pH = 5.8. In contrast, the intensity of the C=O stretch of Asp75 in lipid-reconstituted SR II monolayer does not show such a linear proportionality to the applied voltage. Figure 3 shows a plot of the relative intensity of the C=O stretch of Asp75 (filled circles, intensity normalized to the intensity of the amide I band determined by integrating the area between 1633 and 1666  $\text{cm}^{-1}$ ) versus electrode potential at pH = 5.8. In the potential range  $E > -0.4$  V, where the O intermediate state dominated, the absorption of the C=O stretch of Asp75 is maximum at +0.2 V. This potential corresponds to the open circuit potential (OCP), close to the potential of zero charge (pzc) of the electrode surface.<sup>35</sup> The relative intensity indicated the extent of protonation of Asp75 relative to the conformational changes of the protein backbone. The relative intensity of the C=O stretch of Asp75 decreased both at the positive and the negative side of the pzc (filled circles in Figure 3). This suggests that the proton occupancy at Asp75 is decreased, that is,  $\text{p}K_a$  of Asp75 is lowered, despite the fact that the backbone structural alterations proceeded essentially the same way as in the absence of an electric field. The intensity and the peak position of the amide I (1620–1680  $\text{cm}^{-1}$ ) and the retinal bands (1500–1600  $\text{cm}^{-1}$ ) are invariant toward the applied potential in this potential range. These results suggest that the electric field solely acted on the protonation state of Asp75 without any effect on the backbone or the retinal conformation.<sup>19,20,21</sup>

In the potential region below  $-0.4$  V, where the M intermediate accumulated, the relative intensity of the C=O of Asp75 to the amide I differences is significantly larger as compared to the M–O mixture that is present at  $E > -0.4$  V. However, the C=O stretch of Asp75 in the M state was insensitive in this potential range. Although a slight decrease was observed at very negative potential ( $-0.8$  V), the relative intensity of Asp75 was fairly constant in this potential range (Figure 3, filled circles).

To compare the potential dependency of the M state, the relative intensity of the C=O stretch of Asp75 was plotted versus the potential at pH 7.0 (Figure 3, open triangle). It is evident that the light-induced difference spectra of NpSR II were virtually identical across the applied potential range and

exhibited the vibrational characteristics of the M intermediate. In the potential range above  $-0.4$  V, the intensity of the band of the C=O stretch of Asp75 diminished with decreasing potential. This trend is qualitatively similar to that of the M state in the detergent-reconstituted NpSR II monolayer.<sup>19,20,21</sup> In the potential region below  $-0.4$  V, the intensity of the C=O stretching band of Asp75 increased again as the potential decreased. This tendency was the same as that observed at pH 5.8, while the extent of the change was smaller.

The sensitivity of the C=O stretch of Asp75 to the potential change was more prominent at acidic pH, where the O state predominated, and became negligible at neutral pH, where the M intermediate predominated. This trend is more evident when comparing individual spectra that were recorded under a transmembrane voltage of +0.4 V, +0.2 V,  $-0.3$  V at pH 4.75 and pH 7.5 (Figure 4). As evident from Figure 4A, difference spectra taken at pH 7.5, which reflected the predominant M state, are not susceptible to the applied electric field. In contrast, SEIDA spectra taken at pH 4.75, that is, under conditions that favor the accumulation of the O state, the intensity of the C=O stretch of Asp75 (positive band at 1757  $\text{cm}^{-1}$  in Figure 4B) is much smaller than at pH 7.5 (Figure 4A) or at pH 5.8 (Figure 1). At an applied potential of  $-0.3$  V, however, this band is stronger than at positive potential. At +0.4 V and pH 4.75, small but significant bands appeared at 1712  $\text{cm}^{-1}$  (+) and 1726  $\text{cm}^{-1}$  (–) concomitant to the decreased absorbance at 1757  $\text{cm}^{-1}$ . The positive absorbance change at 1712  $\text{cm}^{-1}$  is interpreted to arise from the C=O stretch of Asp201. The assignment is based on the putative correspondence to bacteriorhodopsin<sup>30,36,37</sup> where the conserved residue, Asp212, relays the proton from Asp85 to the proton release group representing the final proton transfer step in proton translocation by bR.<sup>30</sup> In analogy to bR, we infer that SR II also yields an O-like state with deprotonated Asp75 and protonated Asp201 (O' state).

The pH-dependence of the area of the C=O band of Asp75 is shown in Figure 5 for different applied potentials. At OCP, the relative intensity of Asp75 (Figure 5, open circle) is fairly constant in the pH range from 5.8 to 7.5, that is, at conditions where the M-intermediate predominated. The relative area drops both at positive (+0.4 V, cross) and negative ( $-0.3$  V, closed circle) of OCP at pH 5.8 as observed in Figure 3. Yet, the relative area at both positive and negative increase at elevated pH. At pH 7.0, the relative area of the C=O<sub>Asp75</sub> is almost equal at OCP and at +0.4 V, while it is slightly lower at  $-0.3$  V. This implies that the potential dependency profile of C=O<sub>Asp75</sub> is different from that at pH 5.8, and that the proton occupancy at Asp75 proportionally increases as the potential increases. Finally, the relative area of C=O<sub>Asp75</sub> is almost equal at pH 7.5 for all potentials studied. This result implies that the proton occupancy at Asp75 is independent of the applied electric field at neutral pH.

Under acidic conditions (pH < 5.8), however, the relative area of C=O<sub>Asp75</sub> decreased drastically at OCP and at positive potential (+0.4 V). This finding suggests that proton release from Asp75 in the O' intermediate is promoted by the applied potential when it is more positive. It is interesting to note that the relative area of C=O<sub>Asp75</sub> is even larger at the strongly negative potential ( $-0.3$  V). It is straightforward to conclude

(35) Sondaghuethorst, J. A. M.; Fokkink, L. G. J. *Langmuir* **1995**, *11* (6), 2237–2241.

(36) Zscherp, C.; Schlesinger, R.; Heberle, J. *Biochem. Biophys. Res. Commun.* **2001**, *283* (1), 57–63.

(37) Dioumaev, A. K.; Brown, L. S.; Needleman, R.; Lanyi, J. K. *Biochemistry* **1999**, *38* (31), 10070–10078.

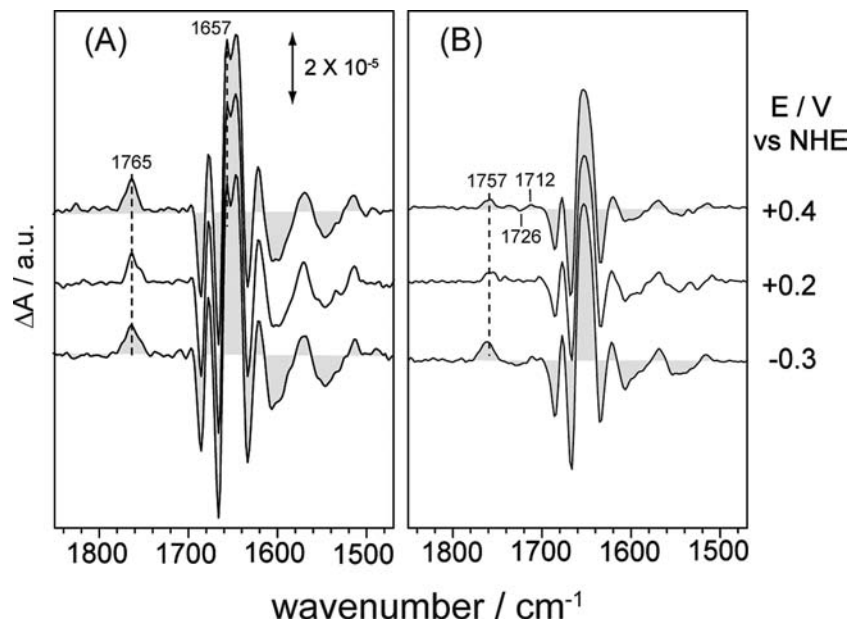


**Figure 4.** Light-induced SEIDA spectra of NpSR II recorded at various potential (top, +0.4 V; middle, +0.2 V; bottom, -0.3 V) and at pH 7.5 (A) and pH 4.75 (B).

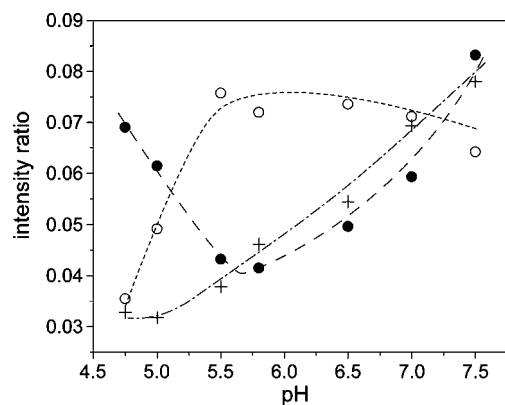


**Figure 5.** Integrated ratio of the C=O stretching vibrational band of Asp75 band at different potentials (cross (+), +0.4 V; open circle (O), +0.2 V; filled circle (●), -0.3 V) plotted versus the solution pH. The intensities of the C=O band is normalized by the integrated band intensity of amide I at 1668–1635  $\text{cm}^{-1}$ .

that deprotonation of Asp75 during O decay was hampered as the potential became negative.

## Discussion

Our vibrational spectroscopic results revealed that the photoreaction of the SR II monolayer is sensitive to the applied electric field. The transition of the difference spectra from the M state to the O state characteristic via the applied potential indicated a regulatory mechanism for the photoreaction. In the following, we will present a molecular view on how the electric field influences the functional changes of the membrane protein.

**Relation between the Potential and pH Dependency of the Spectra.** We found that the light-induced IR difference spectra recorded under the application of an electric field across the SR II monolayer (Figure 1) strongly resembled those light-induced difference spectra recorded at specific pH-values (Figure 2). This fact points to a common physical origin of the influence of the electrode potential and the solvent pH on the functionality of the NpSR II monolayer. Accumulation of the long-lived M

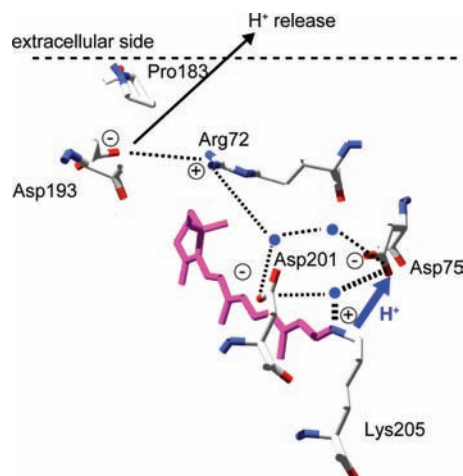


**Figure 6.** Structural model of the amino acid residues of NpSRII lining the proton pathway from the retinal Schiff base to the proton release group. Protons are relocated from the retinal Schiff base via the polar headgroup of aspartic acids (Asp75 and Asp201) and are finally released from Asp193 to the extracellular medium. These polar head groups at the proton pathway form a hydrogen-bonded network including several water molecules (denoted in blue circle). Atomic coordinates have been taken from the RCSB protein data bank (1H68).

intermediate state occurs at  $\text{pH} > 5.8$ , which coincides with proton release at the extracellular surface.<sup>16,38</sup> It has been suggested that  $\text{pK}_a$  of proton release group (PRG) includes Asp193, which is coupled to Asp75 via a hydrogen-bonded network, is lowered and facilitates their proton releasing as resulting in the increase of the  $\text{pK}_a$  of Asp75 to drive the proton translocation from the Schiff base to its counterion in the M state (Figure 6).<sup>16,39</sup> Mutual interaction between PRG and Asp75 favors the accumulation of the M state when deprotonation of the PRG takes place at higher pH. Lowering the pH below 5.8,

(38) Ikeura, Y.; Shimono, K.; Iwamoto, M.; Sudo, Y.; Kamo, N. *Biophys. J.* **2004**, *86* (5), 3112–3120.

(39) Iwamoto, M.; Furutani, Y.; Sudo, Y.; Shimono, K.; Kandori, H.; Kamo, N. *Biophys. J.* **2002**, *83* (2), 1130–1135.



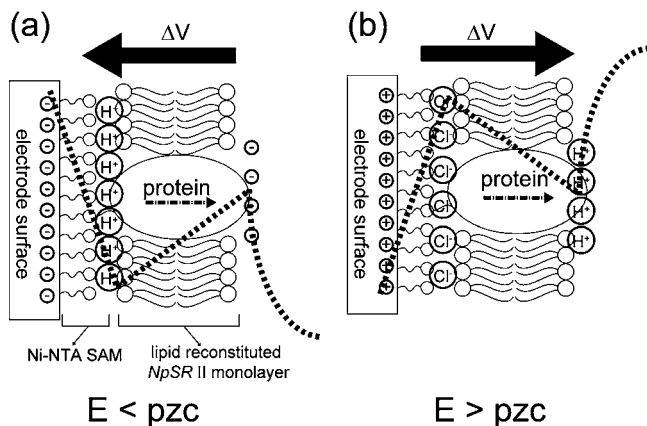


**Figure 7.** Model of the protein monolayer at the solid–liquid interface immersed in the electrochemical double layer. The local potential profile, denoted by dotted line, depends on when the electrode potential is negative of potential of zero charge (pzc) (a) and positive of pzc (b). The bold arrows at the top denote the direction of the net electric fields created by the potential difference between the electrode surface and the bulk electrolyte. The dashed arrows drawn in the protein represent the net direction of proton translocation within NpSR II during the photoinduced reaction cycle.

which leads to protonation of the PRG, causes the domination of the O intermediate under our steady-state conditions. It is known from BR that the fraction of O intermediate increased upon lowering the pH due to decrease of the rate constant of the O to ground state transition at  $\text{pH} < 5$ .<sup>30,40</sup> The PRG is the terminal acceptor in the proton transfer chain from the primary counterion, Asp75 (Asp85 in the case of BR), not only at neutral but also at acidic pH. As a consequence, deprotonation of the counterion can occur only after deprotonation of the PRG.<sup>41</sup> NpSR II lacks the homologous residue of Glu194 of BR, one of major constituents of the PRG in the latter, and is replaced by Pro183. However, fast proton release, which is usually associated with the presence of an intact PRG, is recovered by the addition of  $\text{Cl}^-$  as shown by Iwamoto et al.<sup>42</sup> Analogous to BR, decay of O state in NpSR II coincides with proton transfer from protonated Asp75 to the PRG through an extracellular proton conduction channel, which comprises more hydrophobic residue than in BR.<sup>29</sup> This may be considered as one of the major influences of the slow decay of O intermediate in NpSR II. On the basis of this line of arguments, reprotonation of the PRG represents the determinant in the transition from the O dominated to the M dominated steady-state.

After putting up this model of pH-dependent kinetics of the O state, we now consider the effect of the transmembrane voltage. Since the His-tag was attached to the C-terminus of the protein, the adsorbed SR II monolayer was orientated with the extracellular side facing the bulk aqueous solution. Thus, internal proton transfer proceeds in the direction from the electrode surface toward the solution (see Figure 7, dashed arrow). When the electrode potential is set at negative of the pzc, the net electric field applied across the protein has a direction opposite to proton transfer (Figure 7, solid arrow). When the potential is very negative, for example, at  $E < -0.4$  V, the net charge on the electrode surface becomes negative which leads to the attraction of protons toward the electrode

surface. In turn, the depletion of protons from the diffuse double layer may cause the local pH at the extracellular side of SR II to be significantly higher than that of the bulk, which favors the adsorbed SR II to be in the M predominated state.

**Proton Occupancy at Asp75 Depending on the Electrode Potential in M Intermediate.** Spectra recorded at  $\text{pH} < 7.0$  contain contributions of the O intermediate. Thus, we focus our discussion on the potential dependency of the M intermediate on the spectra at  $\text{pH} > 7.0$ , where the M intermediate state predominated. The spectra at  $\text{pH} 7.0$  showed that the proton occupancy at Asp75 increased when the potential shifts more positive than  $-0.4$  V. This observation is explained in terms of an interaction between the proton and the directional external electric field.<sup>19</sup> In the potential range below  $+0.2$  V, that is, close to pzc, the electrode surface is negatively charged and creates a dipole against the direction of proton translocation from retinal Schiff base to Asp75. As the potential shifts to negative, the energy barrier is sufficiently high to suppress proton translocation in the protein. To produce efficient interaction between the external electric field and the free charge of the proton, the proton pathway should be composed of apolar residues.

When applying very negative potentials ( $E < -0.4$  V), the protonation state of Asp75 in the M state is much less sensitive to the change in potential. Such behavior is reminiscent to the situation when SR II was exposed to alkaline solution ( $\text{pH} > 7.0$ ). As deduced from the similarity between the pH dependence and the potential dependence of the M intermediate, negative potential leads to a significant influence on the protonation state of the PRG; hence, the protonation state of the retinal Schiff base/Asp75 pair is also affected.<sup>41</sup> When the potential was shifted toward very negative potentials, the PRG was deprotonated. This created a polar environment surrounding the retinal Schiff base and Asp75 which may support proton transfer. We infer that the influence of such a polar environment is energetically higher than the external electric field, and hence, the latter cannot exert a significant influence on proton transfer. The gradual increase in proton occupancy of Asp75 at  $E < -0.4$  V may be due to the formation of the polar environment surrounding the ion pair of the retinal Schiff base and Asp75, exceeding the effect of external electric field. Same mechanism can be applied for the potential insensitivity Asp75 at  $\text{pH} 7.5$ . Since this pH is far deviated from  $\text{pK}_a$  of PRG, the polar environment surrounding Asp75, induced by deprotonation of PRG at  $\text{pH} 7.5$ , is already energetically higher than the electric field. Hence, the potential shift cannot influence the protonation state of Asp75.

**The  $\text{pK}_a$  of Asp75 in the O State Depends on the Electrode Potential.** The potential dependence of the O intermediate is different at low pH (4.5 – 5.5) and at almost neutral pH (5.5 – 6.5). In the acidic range, the protonation at Asp75 is small; hence, the  $\text{pK}_a$  of Asp75 is low, at positive potential region. Proton dissociation from Asp75 to the PRG takes place during the decay of the O intermediate.<sup>31</sup> At  $\text{pH} 4.5$ – $5.5$ , the PRG is protonated since the  $\text{pK}_a$  of PRG is 5.7.<sup>38</sup> Protonation of the PRG blocks proton transfer from Asp75; hence, the decay of the O is slowed down. As a consequence, the O state is predominant under these conditions during continuous illumination. When the PRG is protonated, the  $\text{pK}_a$  of Asp75 is downshifted ( $\text{pK}_a = 3.5$ ) compared that in the M state ( $\text{pK}_a = 5.1$ ).<sup>38</sup> Such conditions favor the release of the proton from Asp75, and the released proton is, as a free charge, more sensitive to the external electric field. When the potential is set negative

(40) Cao, Y.; Brown, L. S.; Needleman, R.; Lanyi, J. K. *Biochemistry* **1993**, *32* (38), 10239–10248.

(41) Balashov, S. P. *Biochim. Biophys. Acta* **2000**, *1460* (1), 75–94.

(42) Iwamoto, M.; Furutani, Y.; Kamo, N.; Kandori, H. *Biochemistry* **2003**, *42* (10), 2790–2796.

with respect to the pzc, the electric field vector points opposite to the direction of proton translocation. Under these conditions, the proton transfer will be halted at Asp75. On the other hand, when the potential is more positive than the pzc, proton release from Asp75 is promoted because the electric field parallels the direction of proton translocation. Consequently, the relative intensity of the C=O stretching vibrational band of (protonated) Asp75 becomes smaller (Figure 3). Yet, at pH 4.5, PRG are more protonated, so that the released proton from Asp75 loses its target. Such a situation induced proton release at the extracellular side. However, proton release is not from the initial PRG but from Asp201 that acted as the immediate proton acceptor from Asp75. This assumption is corroborated by the appearance of a vibrational band at  $1712\text{ cm}^{-1}$  (pH 4.5 and  $E = +0.3\text{ V}$ , Figure 4B), which we assign to Asp201 in analogy to Asp212 of BR.<sup>30,37</sup> According to the proton transfer model of BR, Asp201 accepted the proton from Asp75 to form the O' state. This state is hardly accumulated in the absence of the membrane potential because proton translocation from Asp201 to the initial PRG is fast compared to the protonation process of PRG. However, when the proton release from the PRG is suppressed at very low pH, deprotonation of Asp201 is retarded and the C=O stretch at  $1712\text{ cm}^{-1}$  appeared.<sup>30,36</sup> The same effect is achieved by positive electrical potential. Low pH suppresses the proton release from PRG, yet proton release from Asp75 is promoted by the external electric field. This situation halts the proton at Asp201, which normally relays the proton transfer between Asp75 and PRG rapidly. The halted proton at Asp201 is directly released from this site, with the same consequences as a "late proton release process".

It should be noted that  $\text{Cl}^-$  ion binds to PRG under high salt conditions. It has been suggested that these  $\text{Cl}^-$  ions are desorbed when the proton is released from PRG.<sup>29</sup> PRG of NpSR II lacks homologous residue of Glu194 in BR, and is replaced by hydrophobic Pro183. It can be deduced that the adsorption/desorption of  $\text{Cl}^-$  ion on hydrophobic domain of PRG act in a similar role for Glu194 in BR in order to maintain the charge balance of the PRG region and the hydrogen-bonding network in the protein during the proton release. However, the effect of the adsorbed  $\text{Cl}^-$  ion is beyond the scope of this work and further investigation will be necessary.

It may be puzzling that the relative intensity of the C=O stretch of Asp75 was decreasing at less than pzc (pH 5.8, Figure 3). We interpret this observation to be due to the detailed balance between the protonation equilibria of the PRG and Asp75. At a pH of 5.8 which is almost identical to the  $\text{pK}_a$  of PRG, a slight potential shift could affect the protonation state of PRG. When the potential shifts to negative, the local pH surrounding the PRG is increased (vide supra), so that proton translocation from Asp75 to PRG is promoted by the local pH gradient irrespective of the opposite external electric field. As a consequence, the relative intensity of Asp75 is decreased. On the same basis, positive potentials induced proton release from Asp75 due to the directional force from the externally applied electric field, although shift of the local pH induced the slight increase of the proton occupancy at the PRG. Both effects are minimized at the potential of zero charge. As consequence, the slight potential deviation from the pzc serves as driving force for the retraction of proton from Asp75 at pH = 5.8. In other

words, the probability of the proton occupancy at Asp75 becomes maximum at the pzc in pH = 5.8.

## Conclusion

In this work, we have investigated the effect of the membrane potential on the functionality of SR II by applying a voltage drop across the monolayer. It is demonstrated that shifting the electrode potential from positive to negative exerted very similar effects on the photocycle as increasing the pH from acidic to alkaline. This effect is explained in terms of a local pH shift in the vicinity of the membrane surface caused by charge compensation of the potential drop. The proton release groups located at membrane surface were affected by the local pH shift which influenced the kinetics of the photocycle of SR II.

This model can be generalized to the regulation of the enzymatic reaction of membrane proteins. When a potential drop is established across the cellular membrane, counterions, such as protons, are accumulated along the membrane surface to compensate for the extra charge induced by the electric field. Thus, the potential applied between the two electrodes induces a *bona fide* membrane potential ( $\Delta\Psi$ ) across the membrane monolayer comprising electrical ( $\Delta\varphi$ ) as well as chemical potentials ( $\Delta\mu$ ). This shifts the surface pH at the membrane. Protonatable amino acid residues at the membrane surface may be sensitive to such local pH change when their  $\text{pK}_a$  is close to this range. Consequently, these surface residues will be protonated/deprotonated which induces entire rearrangement of the electrostatic charge pattern and/or the hydrogen-bonded network among these residues. Such structural changes inevitably lead to alterations in the functional mechanism, thus, regulating the enzymatic reaction of the protein in response to the membrane potential.

The electric dipole that arises from the potential drop can also act on the movement of an ion that is translocated within the protein. A free charge is easily affected by the direction of the external electric field when immersed in the low dielectric medium of the protein interior. Thus, an action/counter-action between the direction of the movement of the free charge and the directional electric field provides a fine-tuning component for regulation of the enzymatic reaction. On the other hand, if the local hydrogen-bonded network of the protein interior creates a polar environment surrounding the free charge, this may screen the external electric field. Such conditions are achieved when the local pH deviates from the  $\text{pK}_a$  of the local polar residues which leads to ionization. Such polar environment exceeds the effect of the external electric dipole, so that the enzymatic regulation is switched from the external electric effect to local pH driven mechanism.

**Acknowledgment.** K.A. acknowledges financial support by the PRESTO program of the Japan Science and Technology agency. X.J. thanks the Alexander von Humboldt foundation for providing a fellowship. This work was also supported by a grant from the Deutsche Forschungsgemeinschaft (SFB 613, K8) to J.H.

**Supporting Information Available:** We included a direct comparison of two light-induced surface-enhanced infrared difference (SEIDA) spectra of sensory rhodopsin II in reconstituted in halobacterial polar lipids and solubilized in detergent as Figure S1. This material is available free of charge via the Internet at <http://pubs.acs.org>.

JA102295G